University of Nebraska - Lincoln
DigitalCommons@University of Nebraska - Lincoln

USGS Staff -- Published Research | US Geological Survey

1-1-2004

# A mechanical model of the San Andreas fault and SAFOD Pilot Hole stress measurements

Jean Chéry
*Université de Montpellier II*

Mark D. Zoback
*Stanford University*

Stephen Hickman
*U.S. Geological Survey*

Follow this and additional works at: http://digitalcommons.unl.edu/usgsstaffpub

Part of the Earth Sciences Commons

Chéry, Jean; Zoback, Mark D.; and Hickman, Stephen, "A mechanical model of the San Andreas fault and SAFOD Pilot Hole stress measurements" (2004). *USGS Staff -- Published Research.* Paper 398.
http://digitalcommons.unl.edu/usgsstaffpub/398

This Article is brought to you for free and open access by the US Geological Survey at DigitalCommons@University of Nebraska - Lincoln. It has been accepted for inclusion in USGS Staff -- Published Research by an authorized administrator of DigitalCommons@University of Nebraska - Lincoln.

This article is a U.S. government work, and is not subject to copyright in the United States.

# A mechanical model of the San Andreas fault and SAFOD Pilot Hole stress measurements

Jean Chéry
Laboratoire Dynamique de la Lithosphère, Université de Montpellier II, Montpellier, France

Mark D. Zoback
Department of Geophysics, Stanford University, Stanford, California, USA

Stephen Hickman
U.S. Geological Survey, Menlo Park, California, USA

Received 19 January 2004; revised 8 March 2004; accepted 22 March 2004; published 29 July 2004.

[1] Stress measurements made in the SAFOD pilot hole provide an opportunity to study the relation between crustal stress outside the fault zone and the stress state within it using an integrated mechanical model of a transform fault loaded in transpression. The results of this modeling indicate that only a fault model in which the effective friction is very low (<0.1) through the seismogenic thickness of the crust is capable of matching stress measurements made in both the far field and in the SAFOD pilot hole. The stress rotation measured with depth in the SAFOD pilot hole (~28°) appears to be a typical feature of a weak fault embedded in a strong crust and a weak upper mantle with laterally variable heat flow, although our best model predicts less rotation (15°) than observed. Stress magnitudes predicted by our model within the fault zone indicate low shear stress on planes parallel to the fault but a very anomalous mean stress, approximately twice the lithostatic stress. *INDEX TERMS:* 8110 Tectonophysics: Continental tectonics—general (0905); 8123 Tectonophysics: Dynamics, seismotectonics; 8120 Tectonophysics: Dynamics of lithosphere and mantle—general; 8159 Tectonophysics: Rheology—crust and lithosphere 8164 Tectonophysics: Stresses—crust and lithosphere. **Citation:** Chéry, J., M. D. Zoback, and S. Hickman (2004), A mechanical model of the San Andreas fault and SAFOD Pilot Hole stress measurements, *Geophys. Res. Lett.*, *31*, L15S13, doi:10.1029/2004GL019521.

## 1. Introduction

[2] The San Andreas Fault (SAF) has often been discussed as a prototype of a weak plate-bounding fault on the basis of two major arguments: First, no anomalous heat flow is observed near the fault [*Brune et al.*, 1969; *Lachenbruch and Sass*, 1980] which should be present if the fault was characterized by hydrostatic pore pressure and friction coefficients of 0.6–1.0 as measured in the laboratory [*Byerlee*, 1978] and inferred from deep borehole stress measurements in intraplate areas [*Townend and Zoback*, 2000]. Second, stress orientations deduced from earthquake stress inversions and borehole stress measurements along the SAF (mostly at distances of 20–60 km) generally show that the maximum horizontal stress is at a very high angle to the fault trace [*Mount and Suppe*, 1987; *Provost and Houston*, 2003; *Townend and Zoback*, 2004; *Zoback et al.*, 1987]. A variety of hypotheses have been proposed to reconcile these observations, a number of which will be tested in the SAFOD project. The stress data obtained in the SAFOD pilot hole [*Hickman and Zoback*, 2004] represent important new information on the state of stress in the crust immediately adjacent to the SAF. By means of numerical modeling, the goal of this paper is to explore different rheological models of the San Andreas Fault system in central California in terms of both the regional stress field [*Townend and Zoback*, 2004] and the pilot hole stress measurements. Finally, we predict the stress state that may be observed in the fault core at 4 km depth with SAFOD.

## 2. Models

[3] Based on previous numerical experiments [*Chéry et al.*, 2001], we set up our model as a lithospheric cross-section with a 25 km thick crust, a thin upper mantle and a vertical fault zone crossing the entire lithosphere (Figure 1). The whole model is submitted to earth gravity $g$, and an initial lithostatic stress field is assumed (zero initial deviatoric stress). The boundary conditions account for the relative motion between the Pacific plate and the Sierra Nevada, i.e., a moderate convergence velocity (3.5 mm/yr) and a shear velocity of 35 mm/yr. No strain variation occurs along the fault. In accord with heat flow measurements in western California [*Lachenbruch and Sass*, 1980], we utilize a temperature distribution in the model that matches a surface heat flow of ~84 mW/m$^2$ in the Coast Ranges in the vicinity of the fault zone and 40 mW/m$^2$ far from the fault, as is observed in the Central Valley ~40 km east of the SAF in this area. The rheology of the model is elastic-frictional at low temperature and viscoelastic at high temperature. The transition between the two deformation modes is stress-controlled [*Chéry et al.*, 2001]. We used different rheologies for the crust, mantle and fault zone and present results from six numerical experiments (Table 1) to illustrate the effect of different rheological assumptions on the stress field near the SAF and in the adjacent crust.

[4] A common feature of all the models tested is that the crust adjacent to the fault is strong, behaving as a frictional medium with a high coefficient of friction (0.6–0.8) and

Copyright 2004 by the American Geophysical Union.
0094-8276/04/2004GL019521$05.00

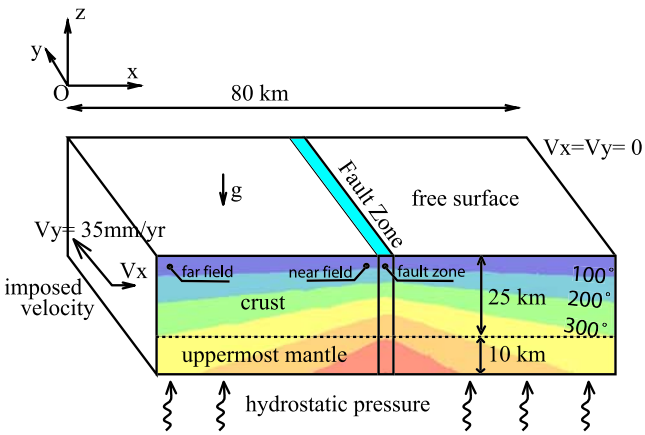


**Figure 1.** Geometry, boundary conditions and initial temperature field for the numerical model. The stress state is assumed to be hydrostatic below a depth of 35 km.

hydrostatic pore pressure [*Townend and Zoback*, 2000]. This rheological state is simulated using an effective friction angle of 15°–20° for a Drucker-Prager criterion [*Chéry et al.*, 2001]. A viscoelastic law (linear Maxwell model) is adopted to fit the strain rate dependent "power law" rheology given by laboratory experiments for crustal and mantle rocks [*Kirby*, 1983]. A quartz-like rheology is used for the viscous lower crust, assuming differential stress levels of ~300 MPa at the brittle-ductile transition [*Kohlstedt et al.*, 1995]. Assuming a typical strain rate of $10^{-15}$ $s^{-1}$ for the middle crust and a strong viscosity decrease with temperature in the lower crust, we adopt a viscosity of $10^{23}$ Pa s at 350°C decaying to a value as low as $10^{20}$ Pa s at 650°C (indicated by the letter Q in Table 1).

[5] Based upon laboratory-derived flow laws for olivine, the rheology of the upper mantle has been viewed as strong for many years [*Brace and Kohlstedt*, 1980]. However, the maximum strength of the continental mantle is a subject of considerable uncertainty [*Karato et al.*, 1986; *Tsenn and Carter*, 1987]. We therefore test models using olivine rheology corresponding to a strong mantle [*Kirby*, 1983] (indicated by Ol in Table 1) and also using a mantle rheology as weak as the crust (indicated by the letter Q in Table 1).

[6] We divide the fault into four depth intervals to allow for different effective friction at shallow (0–5 km), intermediate (5–12 km), deep (12–25 km) and mantle (25–35 km) depths. Effective friction angles of 15° and 3° have been tested to simulate both high and low effective friction in the fault zone, as well as both a quartz rheology (Q) and a weak rheology like mica (M), that has been proposed as governing crustal flow in some highly deformed mid-crustal shear zones [*Gueydan*, 2001; *Wintsch et al.*, 1995]. This weak rheology is modeled using a linear Maxwell model with a low viscosity of $10^{19}$ Pa s.

## 3. Stress Orientation Predictions

[7] Our numerical experiments allow us to compute strain rate and stress tensors throughout the model. We discuss successively stress results in the far field (FF, 40 km away from the fault), in the near field (NF, 2 km from the fault) and in the fault zone (FZ), summarized in Table 1. As shown by [*Townend and Zoback*, 2004] far field stress data in this area indicate that the average orientation of the maximum horizontal principal stress, $S_{Hmax}$ with respect to the fault strike (called β in the following) is 84° (±10°). $S_{Hmax}$ orientations in the SAFOD pilot hole vary with depth increasing from ~35° at 1 ± 0.3 km depth to ~63° at 2 ± 0.2 km depth [*Hickman and Zoback*, 2004]. All numerical experiments involving a low effective friction for nearly the entire fault (cases 1, 2, 3 and 6) yield values of β in the far field between 83° and 87°. Similarly, the observed stress orientation in the pilot hole of ~63° at ~2 km depth is well matched by stress orientations predicted for cases 1, 2 and 6 (63°, 66° and 62°, respectively). Again, each of these cases assumes a very weak SAF to a depth of at least 25 km. Case 4, which assumes a high friction for only the shallow fault also leads to β of 83° in the far field and would thus be consistent with the regional stress data, but is inconsistent with the pilot stress orientations at 2 km depth. Only cases 4 and 5, which assume a high fault friction over some depth interval, lead to a β of about 50° at 2 km, which is markedly different from that observed in the pilot hole. The ~30° rotation of $S_{Hmax}$ with depth in the pilot hole from ~1 km to ~2 km depth is not well reproduced by our model. Only case 2 displays a significant rotation of 15° over this depth interval. As this case also predicts β = 66° for the pilot hole at 2 km depth and β = 87° in the far field it best fits all of the available stress observations. Interestingly, this marked rotation in $S_{Hmax}$ with depth at the pilot hole location appears to be a consequence of the weak rheology (M) assumed for the deep fault zone.

**Table 1.** Rheological Parameters of the Crust, the Mantle, and the Fault Zone (FZ) and Predicted Stress Orientations[a]

| | Rheology | | | | | | Stress Orientations of $S_{Hmax}$ | | | | |
|---|---|---|---|---|---|---|---|---|---|---|---|
| Case | Crust | Mantle | FZ 0–5 km | FZ 5–12 km | FZ 12–25 km | FZ 25–30 km | $\beta_{1\ km}$ | $\beta_{1.5\ km}$ | $\beta_{2\ km}$ | $\beta_{FF}$ | $\beta_2-\beta_1$ |
| 1 | 15/Q | 15/Q | 3/Q | 3/Q | 3/Q | 3/Q | 53 | 63 | 63 | 84 | 10 |
| 2 | 15/Q | 15/Q | 3/Q | 3/Q | 3/**M** | 3/**M** | 51 | 57 | 66 | 87 | 15 |
| 3 | 15/Q | 15/**Ol** | 3/Q | 3/Q | 3/Q | 3/Q | 73 | 73 | 74 | 86 | 1 |
| 4 | 15/Q | 15/Q | **15**/Q | 3/Q | 3/Q | 3/Q | 53 | 52 | 52 | 83 | −1 |
| 5 | 15/Q | 15/Q | 3/Q | **15**/Q | **15**/Q | 3/Q | 45 | 46 | 45 | 48 | 0 |
| 6 | 15/Q | **15/Ol** | 3/Q | 3/Q | 3/Q | **15/Ol** | 57 | 63 | 62 | 83 | 5 |
| Data | | | | | | | 35 | 37 | 63 | 84 | 28 |

[a]Q and Ol refer to viscous rheologies of quartz and olivine, respectively. The modifiers 3 and 15 refer to the friction angle used to describe the superimposed frictional behaviour (3° is approximately equivalent to a friction coefficient of 0.1 and 15° is equivalent to a friction coefficient of 0.6). M means that a constant viscosity of $10^{19}$ Pas is used. Values of β refer to $S_{Hmax}$ orientations predicted in SAFOD pilot hole at 1, 1.5 and 2 km, and in the far field (FF) 40 km away from the fault at 2 km depth.

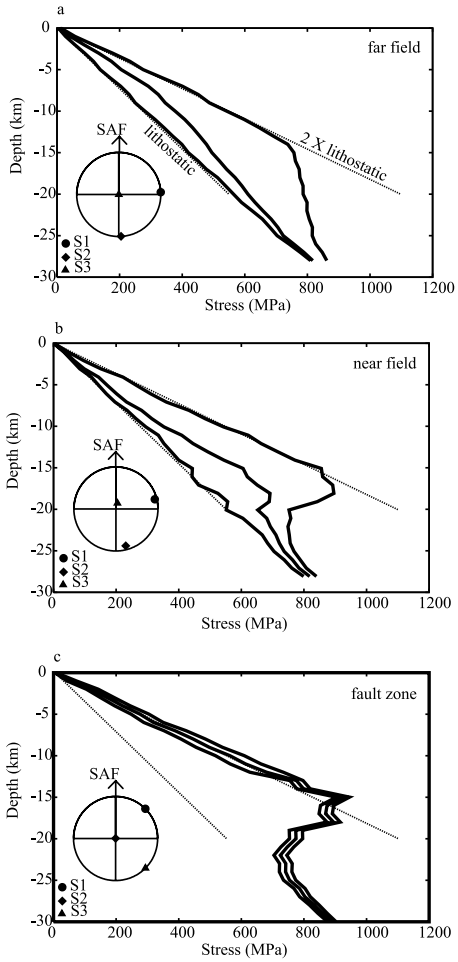


**Figure 2.** $S_1$, $S_2$, $S_3$ profiles with depth and lower hemisphere stereoplots of $S_1$, $S_2$, $S_3$ for case 2 in the far field (a), the near field (b) and in the fault zone (c). The stereoplot is evaluated at 4 km depth and is shown with respect to the strike of the San Andreas Fault, which is shown by an arrow.

[8] The predicted $S_{Hmax}$ orientation directly within the fault zone is 45° for all the cases, consistent with the pure strike slip motion and plastic rheology utilized in the model.

## 4. Stress Magnitude Predictions at SAFOD

[9] Upper crustal stress magnitudes in our model are mostly constrained by the effective friction angle of 15° we chose for the crust adjacent to the fault. In this case, the minimum principal stress, $S_3$ corresponds to the vertical stress. Because $S_2 \sim 0.5\ (S_1 + S_3)$, we find using the Drucker-Prager criterion that $S_1/S_3 = 2$, which is compatible with borehole stress ratios observed in the continental crust [*Townend and Zoback*, 2000]. This stress ratio of 2 is observed at both far-field and near-field locations (Figures 2a and 2b), indicating that the crust is on the verge of failure in a strike-slip/reverse faulting regime throughout the Coast Ranges. At such locations, the minimum stress is close to the lithostatic stress, which corresponds in our model to $\rho gh$ ($\rho$ being the crustal density and $h$ the depth below the surface). Note how similar the stress state shown in Figure 2b is to that reported to a depth of about 2 km for the pilot hole [*Hickman and Zoback*, 2004]. The minimum and maximum principal stresses are in a vertical plane almost perpendicular to the SAF direction. Therefore, corresponding localized deformation occurs as almost pure thrusting on faults striking parallel to the SAF. This stress state is fairly consistent with Quaternary deformation of anticlines 30–50 km east of the SAF and with a model of partitioned strain [*Mount and Suppe*, 1987]. Because $S_1$ is at a high angle to the SAF trace, stress equilibrium implies that the normal stress acting on the fault zone ($S_{xx}$) is close to $S_1$. This has drastic implications for the stress state within the fault zone (Figure 2c), in which all three principal stresses are predicted to be close to two times lithostatic stress (as is the mean stress, defined by 1/3 ($S_1 + S_2 + S_3$)). This prediction, which is consistent with the state of stress predicted by *Rice* [1992], means that the ratio of $S_3$ to the lithostatic stress should increase dramatically between the pilot hole and the core of the SAF, changing from a value of 1 to 2 in only about 1.5–2 km of horizontal distance. Such a stress variation will be readily detectable with stress measurements planned across the fault zone with SAFOD.

[10] We now examine how $\beta$ varies throughout the lithosphere for case 2 (Figure 3). Apart from the fault zone where $\beta$ is constant with depth (and equal to 45°), three zones can be identified. First, a high angle zone ($\beta > 80°$) in the upper crust (0–15 km depth) at some distance (15 km) from the fault trace and also in the mid-crust (10–20 km) close to the fault. Second, a shallow zone (0–8 km) in the vicinity of the SAF where $\beta$ is moderately high (40–80°) and increases montonically with depth. Third, a zone at depths below 20 km where $\beta$ has intermediate (50–80°) values.

## 5. Shear Stress on the SAF

[11] We used our model to study the depth variation in shear stress $S_{xy}$ (called hereafter $\tau$) resolved onto planes parallel to the SAF within the fault zone for case 2 (Figure 4), which replicates best both the pilot hole and far field stress orientations. In the fault zone, $\tau$ increases linearly to 40 MPa at 12 km depth, then drops rapidly to about 20 MPa in the low viscosity zone in the mid and lower crust. Thus the average shear stress acting on the SAF is ~20 MPa, which is consistent with the upper bound permitted by heat flow data in the vicinity of the SAF [*Lachenbruch and Sass*, 1980].

[12] Case 2, our preferred model, is in reasonably good agreement with stress orientation and magnitude measurements in the SAFOD pilot hole and stress orientation (and

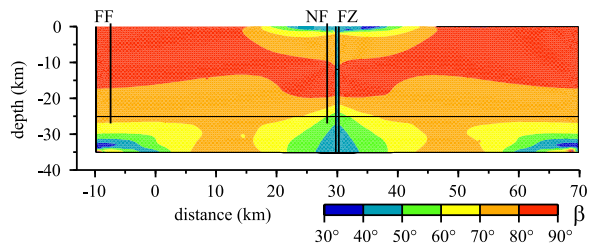


**Figure 3.** $S_{Hmax}$ orientation with respect to the strike of the San Andreas Fault ($\beta$) for case 2. FF and NF denote the far field and near field locations (see Figure 2); FZ is the San Andreas Fault Zone.

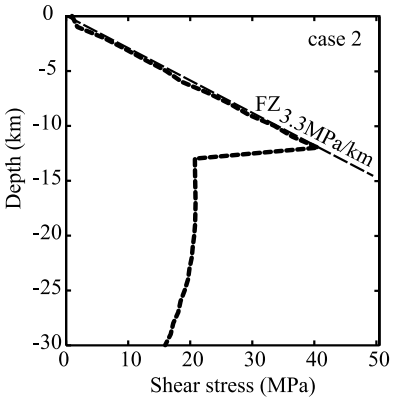


**Figure 4.** Shear stress $\tau$ acting parallel to the San Andreas Fault within the fault zone as a function of depth for case 2.

relative magnitude data) at greater distances from the SAF in central California. The predicted stress state within the fault zone (and the adjacent crust) is also in broad agreement with the mechanical model of *Rice* [1992]. However, stress orientations in our model - and, hence, shear stress resolved onto planes parallel to the SAF - strongly vary with distance to the fault and with depth (Figure 3). These variations were not present in Rice's model, which was constructed assuming a homogeneous half-space with an embedded fault. As shown by previous models [*Chéry et al.*, 2001], these lateral shear stress variations occur in response to a lateral rheological contrast in the crust. In the far field, a cold and strong lithosphere supports higher differential stress at depth while, in the near field, a higher heat flow forces higher differential stress to be mainly restricted above 20 km.

## 6. Discussion

[13] Stress orientation and heat flow data in the vicinity of the SAF in central California can be explained by a limited range of models. High measured angles between $S_{Hmax}$ and the SAF in the far field (i.e., $\beta > 80°$) can be reproduced if the SAF is weak throughout the crust, although a high effective friction (0.6) along the shallow part of the SAF (i.e., a strong fault from 0–5 km) is also compatible with far-field $S_{Hmax}$ orientations ($\beta = 83°$). Stresses observed in the SAFOD pilot hole add the important dual constraints of $S_{Hmax}$ at about 63° to the SAF at ~2 km depth and a large $S_{Hmax}$ rotation between 1 and 2 km depth [*Hickman and Zoback*, 2004]. Only models having a small effective friction on the entire SAF reproduce these features, although none of the models tested were able to reproduce the magnitude of the stress rotation observed in the pilot hole (~30°). Surprisingly, mantle rheology has a clear effect on shallow stress rotation, and a strong mantle rheology has the effect of reducing the magnitude of the predicted $S_{Hmax}$ rotation. Such a relation could be of prime importance in establishing the differential stress magnitudes in the uppermost mantle. Therefore, extensive numerical experiments, including various thermal fields and non-linear viscous rheologies need to be performed to further investigate the mechanical link between the mantle and the crust.

[14] Also, the influence of boundary conditions on the stress field needs to be more fully explored. While shortening along the x-direction - corresponding to formation of the Transverse Ranges and Coast Ranges - is clearly responsible for the reverse faulting stress state adjacent to the SAF, possible strain variations parallel to strike of the SAF are not accounted for our model and should be investigated. For example, slight variations in $\varepsilon_{yy}$ along strike might lead to variations in the magnitude of $S_2$ relative to $S_1$ and $S_3$.

[15] In conclusion, while other (perhaps local) factors may contribute to the magnitude of the stress rotation observed in the pilot hole, the most important finding of our model is that $S_{Hmax}$ orientations observed near the bottom of the SAFOD pilot hole and the occurrence of a clockwise stress rotation in the pilot hole with depth are fully compatible with a very weak fault (friction about 10 times smaller than crustal friction) embedded in a strong crust and weak upper mantle. In central California, the rotation in $S_{Hmax}$ from very high angles to the SAF in the far field (>80°) to moderately high angles in the near field (~63° at 2 km depth in the pilot hole) is also compatible with stress orientation deduced from earthquakes near the SAF in southern California [*Townend and Zoback*, 2004] and precludes the large stress rotations of ~45° in the vicinity of the SAF predicted by strong SAF/strong crust models such as that of [*Scholz*, 2000]. Apart from stress rotations, our model also predicts that the magnitude of the minimum principal stress in the core of the SAF is about two times lithostatic. The SAFOD project will provide additional stress data from greater depth and directly within the San Andreas Fault Zone, making it possible to further constrain this and other model predictions.

[16] **Acknowledgments.** We thank two anonymous reviewers who provide helpful reviews. Mark Zoback would like to acknowledge National Science Foundation support through grant 0208493. Stephen Hickman was supported by the U.S. Geological Survey's Earthquake Hazards Program.

## References

Brace, W. F., and D. L. Kohlstedt (1980), Limits on lithospheric stress imposed by laboratory experiments, *J. Geophys. Res.*, *85*, 6248–6252.
Brune, J. N., T. L. Henyey, and R. F. Roy (1969), Heat flow, stress, and rate of slip along the San Andreas Fault, California, *J. Geophys. Res.*, *74*, 3821–3827.
Byerlee, J. D. (1978), Friction of rock, *Pure Appl. Geophys.*, *116*, 615–626.
Chéry, J., M. D. Zoback, and R. Hassani (2001), An integrated mechanical model of the San Andreas Fault in central and northern California, *J. Geophys. Res.*, *106*, 22,051–22,066.
Gueydan, F. (2001), The brittle-ductile transition of the extending continental crust: Field study and mechanical modelling, Ph.D. thesis, Univ. Paris 6, Paris, France.
Hickman, S., and M. D. Zoback (2004), Stress orientations and magnitudes in the SAFOD Pilot Hole, *Geophys. Res. Lett.*, *31*, L15S12, doi:10.1029/2004GL020043.
Karato, S. H., M. S. Paterson, and J. D. Fitzgerald (1986), Rheology of synthetic olivine aggregates: Influence of grain size and water, *J. Geophys. Res.*, *91*, 8151–8176.
Kirby, S. (1983), Rheology of the lithosphere, *Rev. Geophys.*, *21*, 1458–1487.
Kohlstedt, D. L., B. Evans, and S. J. Mackwell (1995), Strength of the lithosphere: Constraints imposed by laboratory experiments, *J. Geophys. Res.*, *100*, 17,587–17,602.
Lachenbruch, A. H., and J. H. Sass (1980), Heat flow and energetics of the San Andreas fault zone, *J. Geophys. Res.*, *85*, 6185–6223.
Mount, V. S., and J. Suppe (1987), State of stress near the San Andreas fault: Implications for wrench tectonics, *Geology*, *15*, 1143–1146.
Provost, A.-S., and H. Houston (2003), Stress orientations in northern and central California: Evidence for the evolution of frictional strength along

the San Andreas plate boundary system, *J. Geophys. Res.*, *108*(B3), 2175, doi:10.1029/2001JB001123.

Rice, J. R. (1992), Fault stress states, pore pressure distributions, and the weakness of the San Andreas fault, in *Fault Mechanics and Transport Properties of Rock: A Festschrift in Honor of W. F. Brace*, edited by B. Evans and T.-F. Wong, pp. 475–503, Academic, San Diego, Calif.

Scholz, C. H. (2000), Evidence for a strong San Andreas fault, *Geology*, *28*, 163–166.

Townend, J., and M. D. Zoback (2000), How faulting keeps the crust strong, *Geology*, *28*, 399–402.

Townend, J., and M. D. Zoback (2004), Regional tectonic stress near the San Andreas fault in central and southern California, *Geophys. Res. Lett.*, *31*, L15S11, doi:10.1029/2003GL018918.

Tsenn, M. C., and N. L. Carter (1987), Upper limits of power law creep of rocks, *Tectonophysics*, *136*, 1–26.

Wintsch, R. P., R. Christoffersen, and A. K. Kronenberg (1995), Fluid-rock reaction weakening of fault zones, *J. Geophys. Res.*, *100*, 13,021–13,032.

Zoback, M. D., et al. (1987), New evidence on the state of stress of the San Andreas fault system, *Science*, *238*, 1105–1111.

J. Chéry, Laboratoire Dynamique de la Lithosphère, CC 060, Université de Montpellier 2, F-34095 Montpellier, France. (jean@dstu.univ-montp2.fr)

M. D. Zoback, Department of Geophysics, Stanford University, Stanford, CA 94305, USA.

S. Hickman, U.S. Geological Survey, 345 Middlefield Road, MS 977, Menlo Park, CA 94025, USA.